Linear and Quasi-Linear Viscoelastic Characterization of Ankle Ligaments

J. R. Funk
G. W. Hall
J. R. Crandall
W. D. Pilkey
Automobile Safety Laboratory,
Department of Mechanical, Nuclear, and
Aerospace Engineering,
University of Virginia,
Charlottesville, VA 22903

The objective of this study was to produce linear and nonlinear viscoelastic models of eight major ligaments in the human ankle/foot complex for use in computer models of the lower extremity. The ligaments included in this study were the anterior talofibular (ATaF), anterior tibiofibular (ATiF), anterior tibiotalar (ATT), calcaneofibular (CF), posterior talofibular (PTaF), posterior tibiofibular (PTiF), posterior tibiotalar (PTT), and tibiocalcaneal (TiC) ligaments. Step relaxation and ramp tests were performed. Back-extrapolation was used to correct for vibration effects and the error introduced by the finite rise time in step relaxation tests. Ligament behavior was found to be nonlinear viscoelastic, but could be adequately modeled up to 15 percent strain using Fung's quasilinear viscoelastic (QLV) model. Failure properties and the effects of preconditioning were also examined. [S0148-0731(00)01001-3]

Introduction

Much has been written about the viscoelasticity of soft tissues in general [1,2] as well as ligaments in particular (canine MCL: [3]; rabbit MCL: [4,5]; human MCL: [6]; human ACL: [7]; human coracoacrimonial ligament: [8]; human lumbar spine ligaments: [9]). However, prior research on ankle ligaments has focused on quantifying their ultimate strength [10–12], particularly for the lateral ankle ligaments, since they are the most commonly injured. Previous researchers have used a variety of displacement rates to fail ankle ligaments, ranging from quasi-static (0.53 mm/s) [11] to dynamic (1000 mm/s) [10]. A few studies [10,11] have presented stiffness constants for ankle ligaments, implicitly modeling the ligament as a linear elastic spring. Although nonlinear and viscoelastic behavior in ankle ligaments has been observed [10], no viscoelastic model for any ankle ligament has been published, to our knowledge.

Injuries to the ankle are common and debilitating [13]. Numerous studies have looked at ankle injuries both experimentally [14,15] and with computational models [16–19]. Computational modeling has the advantage of being a low-cost, flexible way to study ankle kinematics and injury. Many current lower extremity models lump the effects of ankle ligaments into joint properties, and therefore cannot predict injuries to individual ligamentous structures [20,21]. Models that do include individual ankle ligaments in the geometry are limited to elastic models of ligament behavior [19,22,17]. However, the viscoelasticity of a tissue's mechanical response is an important aspect of its physiological function [23]. The lower extremity MADYMO model by Hall et al. [16] includes viscoelastic ankle ligaments based on data presented here.

The eight ligaments chosen for this study represent the major ligamentous structures affecting ankle joint motion (Fig. 1). The ATT, TiC, and PTT ligaments comprise the deltoid, which is a triangular fan of fibers originating at the medial malleolus that stabilizes the ankle joint on the medial side. The ATaF, CF, and PTaF ligaments stabilize the ankle joint on the lateral side. The ATaF ligament is the most commonly injured ligament in lateral ankle sprains, followed by the CF ligament [24]. The ATiF and PTiF ligaments are very stiff ligaments that comprise the distal syndesmosis and stabilize the ankle mortise. Injury to these ligaments is known as a ''high ankle sprain'' and is associated with prolonged disability [25].

Theory

In viscoelastic theory, constitutive equations are usually formulated in terms of stress and strain. However, this paper presents experimental data in terms of force F and displacement x, which is normalized to engineering strain $\varepsilon = x/L_0$, where L_0 is the initial length. All formulations presented here are therefore in terms of force and engineering strain. The force response of a material to a step input in strain is given by the relaxation function of that material, $R(t)$. The relaxation function $R(t)$ can be used to calculate the force response of a linear viscoelastic material over an arbitrary strain history by applying Boltzmann's principle of superposition. The result is the hereditary integral [2]:

$$F(t) = \int_{-\infty}^{t} R(t-\tau)\frac{d\varepsilon(\tau)}{d\tau}d\tau$$

A linear viscoelastic model can be represented by a discrete combination of springs and dashpots that model the elastic and viscous components of the material, respectively. A common linear viscoelastic model that approximates ligament force-relaxation be-

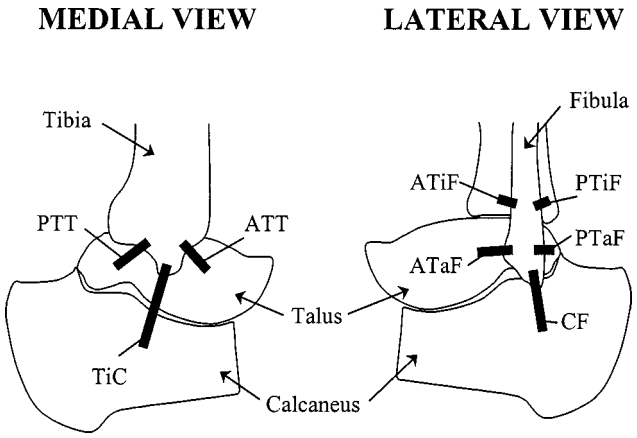

Fig. 1 Locations of the eight major ankle ligaments examined in this study

Contributed by the Bioengineering Division for publication in the JOURNAL OF BIOMECHANICAL ENGINEERING. Manuscript received by the Bioengineering Division April 23, 1998; revised manuscript received September 5, 1999. Associate Technical Editor: R. Vanderby, Jr.

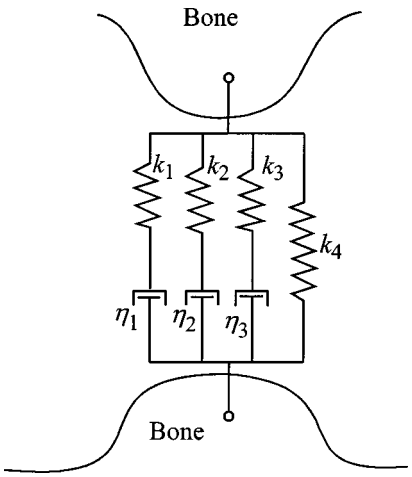

Fig. 2 Spring-dashpot model of an ankle ligament

havior (finite peak force response that decays to a nonzero value) is the generalized Maxwell model [26]. For example, the force relaxation response to a step displacement x for the generalized Maxwell model shown in Fig. 2 is given by

$$R(x,\ t)=\left[k_1 \exp\frac{-k_1 t}{\eta_1}+k_2 \exp\frac{-k_2 t}{\eta_2}+k_3 \exp\frac{-k_3 t}{\eta_3}+k_4\right]\cdot x$$

The linear model has the advantage of being simple and convenient to use in many computer modeling packages.

Although most biological materials are expected to behave linearly for small deformations (<2–3 percent), biological materials typically exhibit nonlinear behavior at greater strains. Many nonlinear viscoelastic models have been formulated, but Fung's theory of quasi-linear viscoelasticity (QLV) is probably the most widely used due to its simplicity. Fung's QLV theory assumes that a material's response can be separated into strain-dependent and time-dependent components [2]. Fung formulates the relaxation function of a quasi-linear viscoelastic material as:

$$R(\varepsilon,\ t)=G(t)\cdot T(\varepsilon)$$

where $G(t)$ is the reduced relaxation function normalized by the peak force or stress value, and $T(\varepsilon)$ is called the instantaneous elastic response function, which may be nonlinear. Assuming that the principle of superposition remains valid, the hereditary integral for a quasi-linear viscoelastic material takes the form

$$F(t)=\int_{-\infty}^{t} G(t-\tau)\frac{fT[\varepsilon(\tau)]}{f\varepsilon}\frac{f\varepsilon(\tau)}{f\tau}d\tau$$

In practice, functions for $T(\varepsilon)$ and $G(t)$ are obtained by curve-fitting experimental data. It is physically impossible to obtain these functions precisely, because they require experimental data from an instantaneously applied step. In reality, a step function is more like a ramp with a finite rise time. Typically, the rise time is ignored, and the relaxation function $G(t)$ is calculated by defining the time of peak force response as $t=0$. Because the portion of the relaxation function between time zero and the rise time t_r cannot be determined, it is desirable to minimize the rise time as much as possible, so as not to lose information pertaining to very short time constants less than t_r. Likewise, it is not possible to continue a step relaxation test for an infinite period of time, and the point at which the step relaxation test is ended is commonly approximated as infinite time. It is therefore desirable to continue step relaxation tests for as long as possible so as not to lose information about very long time constants beyond the hold time of the test.

The elastic response function $T(\varepsilon)$ is also subject to experimental error due to the inability of experimental testing equipment to perform an instantaneous step test. Often, $T(\varepsilon)$ is approximated from the stress versus strain response during the ramp portion of a step test. $T(\varepsilon)$ can also be approximated by curve-fitting the stress-strain isochrone at time zero from the peak stress values seen in step tests or cyclic tests of various strain magnitudes [27].

The linearity of a material can be evaluated by plotting the elastic function at the strain levels of interest. A high degree of nonlinearity in the elastic function indicates that a linear model may not be appropriate. For a material to be considered linear viscoelastic, it must not only exhibit linearity in the spatial domain, but it must also have a characteristic reduced relaxation function $G(t)$ that is independent of strain level. The strain independence of the reduced relaxation function is a result of the application of the Boltzmann principle of superposition, and is therefore a necessary, though not sufficient, condition for a material's behavior to be described as either linear or quasi-linear. The principle of superposition holds over the range of strain magnitudes in which the reduced relaxation functions are the same. If the reduced relaxation function of a material is not strain independent at the strain levels of interest, then a fully nonlinear viscoelastic model, such as the multiple integral formulation proposed by Green and Rivlin [28], may be necessary to describe the material. Unfortunately, fully nonlinear models are extremely complex, require the experimental determination of an unwieldy number of constants, and usually cannot be implemented in standard computer modeling software. The quasi-linear model has the advantage of being simpler than a nonlinear model, more accurate than a linear model for most biological materials, and suitable for computer models that allow nonlinear spring and dashpot functions.

Methods

Specimen Preparation. Three pairs of below-knee amputation specimens were acquired from male donors, ages 45, 47, and 58. The individuals had no record of joint disease or injury. Specimens were used in accordance with local and federal laws pertaining to cadaveric testing. The specimens were frozen within one week postmortem and were thawed for 24 hours prior to dissection. Although stature and body mass were unknown for two of the donors, one donor was 5′10″ tall and 187 lb., which is comparable to the size of a 50th percentile male [29]. The foot lengths of the other two donors were measured to be 26 cm and 27.5 cm, which are comparable to the foot length of a 50th percentile male, 26.9 cm [29].

Twenty-nine (29) bone-ligament-bone specimens were harvested from the six foot/ankle complexes. It was not possible to dissect out bone-ligament-bone specimens for all eight ligaments of interest from each foot/ankle, due to their proximity to each other. Two dissection schemes were developed to maximize ligament yield: one that obtained four ligaments and one that obtained six ligaments. The dissection process involved sectioning bones into halves or quadrants, which may have weakened the bone ends to the point that they failed at lower loads than they otherwise would have during failure testing. This limitation was deemed acceptable since the ultimate strengths of many of the ligaments have already been reported [12,10], and because the intent of this study was to focus on the subfailure viscoelastic properties of the ligaments.

For each pair of limbs, the calcaneofibular (CF), anterior tibiofibular (ATiF), posterior tibiofibular (PTiF), and tibiocalcaneal (TiC) ligaments were harvested from one limb, while the anterior talofibular (ATaF), posterior talofibular (PTaF), anterior tibiotalar (ATT), posterior tibiotalar (PTT), ATiF, and PTiF ligaments were harvested from the contralateral limb. The sample size for the ATiF and PTiF ligaments was therefore twice as large ($n=6$) as the sample size of the other six ligaments ($n=3$). One PTiF ligament was damaged during the dissection process and could not be used for testing. After dissection, the bone-ligament-bone specimens were frozen and stored at −4°C. All specimens were tested within one week of dissection.

Testing Protocol. On the day of testing, specimens were thawed, and the relaxed lengths of the ligaments were measured with calipers. Due to difficulties encountered in measuring the cross-sectional dimensions of the very soft ligaments, force data could not be normalized by cross-sectional area. However, force was deemed the parameter of greatest interest. In the future, it may be possible to scale the force data to stress if ligament cross-sectional area can be related to some other anthropometric parameter, such as ligament length or body size. The bone ends were mounted in aluminum potting cups using a low melting point alloy (Ceralow™, 158°F). The bone ends were placed in the potting cups such that the in vivo anatomical orientation of the bone-ligament-bone complex was maintained, and the long axis of the ligament was oriented along the direction of loading of the test machine (Fig. 3). Several 1/8 in. holes were drilled in the bone ends to allow the potting material to permeate the bone and form a more effective mechanical interlock. The heated metal was then poured into the cup and allowed to cool around the bone end. Potted bone-ligament-bone specimens were then wrapped in gauze soaked in phosphate-buffered saline (PBS, pH 7.4), placed in a servo-hydraulic materials testing machine (MTS 858 Bionix, Eden Prairie, MN) and subjected to a battery of viscoelastic characterization tests (Fig. 4).

Ligament zero strain was defined by pretensioning the specimen until it began to resist with a nominal load (2 N) [12,7,30,8,4]. First, the unpreconditioned ligament was subjected to a step relaxation test (~180 mm/s) up to the level of maximum strain. Initially the maximum strain value was chosen to be 10 percent, because it was believed that none of the ligaments would yield or fail at 10 percent strain. As testing progressed, it was noted that a 10 percent step strain often produced very low loads in the ligament, so the maximum strain level was raised to 20 percent. No damage was apparent in the ligaments after testing to 20 percent strain. The step strain test continued until force relaxation appeared complete or 1000 s had elapsed [23]. The ligament was allowed to recover at zero strain for a period of time greater than the force relaxation time.

The ligament was then preconditioned by applying 10 step strains up to the level of maximum strain and back down to zero strain. The preconditioned ligament then underwent a battery of five successive force relaxation tests at strain levels of 10, 8, 6, 4, and 2 percent strain, or 20, 15, 10, and 5 percent strain. For at least one sample of each ligament type, every step strain was held for 1000 s. For other samples, only the step at the maximum strain level was held for the entire relaxation time, while the smaller step strains were held for 10 s to reduce testing time. In all cases, the ligament was allowed to recover at no load for the full relaxation time between steps and afterward. For some samples, after the final step test, a series of triangle waves at varying strain rates (1/s, 0.1/s, and 0.01/s) were applied up to the maximum strain and back down. The ligament was allowed to recover at no load between triangle waves and afterwards. All samples were subjected to a final failure test (~280 mm/s). Step tests were applied at the maximum rate attainable by the test machine. Due to the deceleration associated with stopping the crosshead at a given step displacement, the machine was able to attain a higher rate for the failure tests (~280 mm/s) than the step and hold tests (~180 mm/s).

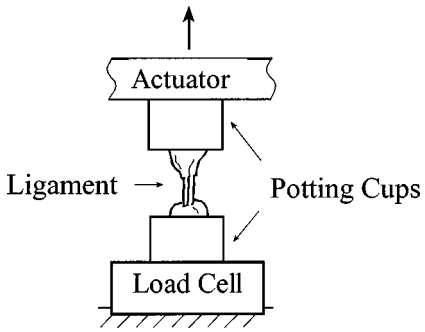

Fig. 3 Specimen mounting scheme

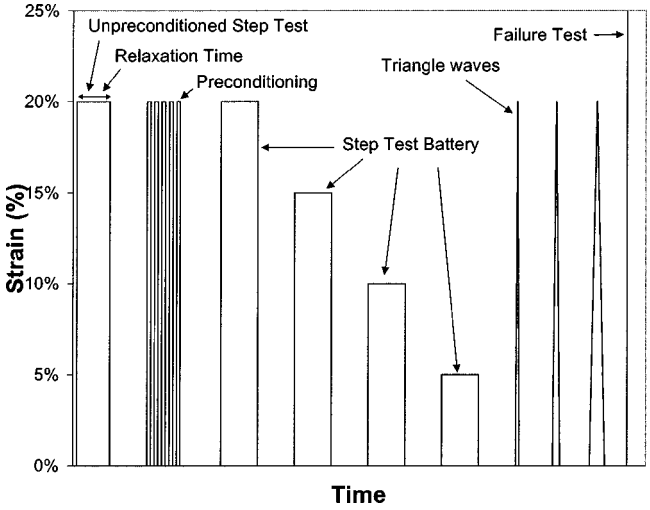

Fig. 4 Schematic illustrating all possible phases of the test battery applied to ligament specimens

Data Processing. For each step test, load, displacement, and time data were recorded at 1000 Hz for the first one second, then at 10 Hz thereafter to reduce file size. Time zero was defined as the initial rise in displacement. Based on the observation that a large, oscillating shock wave occurred as an immediate response to the step displacement, force data for the first 0.1 s after time zero were deemed artifactual and ignored. The artifactual nature of the shock wave was confirmed by performing a Fast Fourier Transform (FFT) on data from step tests with and without a specimen in the machine. In both cases, peaks were seen near the frequency of 20 Hz, which was the frequency seen in the shock wave and likely represents the natural frequency of the test machine. Mechanical vibrations have been known to contaminate data from step tests [27], but in this case, the shock wave appeared almost completely damped out 0.1 s after the initial rise in displacement. For all step tests, the relaxation function was regressed

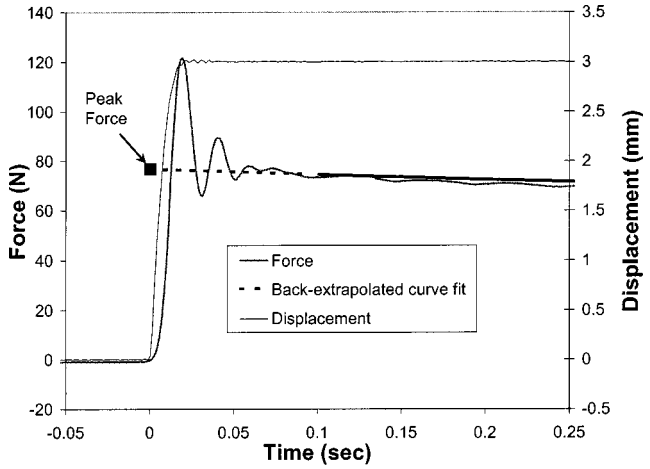

Fig. 5 Example of the large shock wave vibrations seen in step tests. The curve fit of the relaxation function is shown with the back-extrapolated portion (0 s<t<0.1 s) indicated by the dashed line.

to data beginning at time 0.1 s and back-extrapolated to time zero. Peak force values were taken as the back-extrapolated value at time zero (Fig. 5).

Reduced relaxation functions were obtained by normalizing the relaxation data by the peak force value. All curve-fitting was performed using a standard statistical software package (NCSS '97). Several equation forms were fit to a few sample reduced relaxation functions in order to determine how many exponentials would be necessary to achieve a good fit. It was found that a single exponential did not produce a very good fit. Two exponentials produced a very good fit as measured by the coefficient of determination R^2 ($R^2 \sim 0.99$), but the fit was not always good when visually inspected. Three exponentials produced an excellent fit both statistically ($R^2 \sim 0.999$) and visually. No appreciable gain in accuracy was achieved by extending the equation form to more than three exponentials, so the final equation form for the reduced relaxation function curve-fit was chosen to be

$$G_r(t) = G_1 e^{-t/\tau_1} + G_2 e^{-t/\tau_2} + G_3 e^{-t/\tau_3} + G_\infty$$

For specimens where multiple relaxation time histories were obtained at different strain levels, a single reduced relaxation function was obtained by curve-fitting all of the reduced relaxation output data from the multiple tests. It was found that curve-fitting all of the time histories produced the same coefficients as curve-fitting a point by point mean of each of the time histories (although the R^2 values were different). The goodness of fit as measured by the coefficient of determination R^2 was therefore one method used to assess the validity of the principle of superposition at those strain levels. The strain dependence of the reduced relaxation functions was further analyzed by comparing G_∞ values for reduced relaxation functions at different strain levels. Values of G_∞ were compared statistically using a two-tailed, paired sample t test for means (significance level of $p < 0.05$). For each ligament type, data from the reduced relaxation functions for each specimen were combined and curve-fit together. The goodness of fit as measured by the coefficient of determination R^2 was used to assess the interspecimen variability for each ligament type.

The elastic response function $T(\varepsilon)$ was obtained by regressing the force-strain isochrone at time zero for each sample. Data points were curve-fit to the commonly used equation form [31,32,3]:

$$T(\varepsilon) = A(e^{B\varepsilon} - 1)$$

The coefficient of determination R^2 was again used to assess interspecimen variability.

In addition to producing viscoelastic models of ankle ligaments at subfailure levels, this study also examined failure characteristics and some other viscoelastic properties of ankle ligaments. Failure data obtained from these tests were compared to values in the literature. Hysteresis loops were obtained from the responses of specimens to triangular waves applied at strain rates spanning three decades. The effects of preconditioning were evaluated by comparing the step response of specimens in the unpreconditioned state to their step responses after preconditioning.

Results

Curve-Fits. Reduced relaxation functions from individual specimens that were curve-fit to three exponentials plus a constant were found to have an excellent goodness of fit ($R^2 > 0.99$ in most cases). However, interspecimen variability in the reduced relaxation functions of a given ligament type was found to be relatively high (average $R^2 = 0.655$) (Table 1) (Fig. 6). Nevertheless, mean reduced relaxation functions were quite similar between ligament types. Average long-time (1000 s) relaxation was between 44 and 73 percent (mean 61.7 ± 9.7 percent) of the peak force for the eight ligament types tested. In addition, time constants of the mean reduced relaxation functions were generally similar for all ligament types and over an order of magnitude apart (approximately 0.5 s, 10 s, and 200 s) (Table 1).

Table 1 Reduced relaxation function curve fit data

Ligament	sample size	G_1	τ_1 (sec)	G_2	τ_2 (sec)	G_3	τ_3 (sec)	G_∞	R^2
ATaF	n=3	0.092	0.558	0.104	8.51	0.144	132.8	0.661	0.536
ATiF	n=6	0.091	0.627	0.100	11.11	0.158	217.1	0.651	0.603
ATT	n=3	0.091	0.465	0.084	6.95	0.097	131.8	0.729	0.422
CF	n=3	0.069	0.605	0.073	12.72	0.209	244.1	0.649	0.680
PTaF	n=3	0.078	0.472	0.081	9.48	0.146	185.2	0.695	0.620
PTiF	n=5	0.097	0.765	0.112	12.86	0.189	161.1	0.602	0.793
PTT	n=3	0.127	0.832	0.152	14.75	0.284	216.9	0.438	0.918
TiC	n=3	0.125	0.704	0.152	11.16	0.209	164.6	0.514	0.664

Curve-fits of the elastic response function $T(\varepsilon)$ for individual specimens were found to have an excellent goodness of fit ($R^2 > 0.99$ in most cases). Interspecimen variability differed depending on the ligament type, but was generally good. The elastic responses of the ATaF, ATT, PTaF, and PTT ligaments were found to be extremely consistent among specimens ($R^2 > 0.96$) (Table 2). Interspecimen variability was somewhat higher for the ATiF and CF ligaments ($R^2 > 0.75$), and very high for the PTiF and TiC ligaments ($R^2 < 0.6$). The elastic response varied greatly among ligament types. Due to the nonlinear form of the elastic function, it is difficult to rank the ligament types in order of relative stiffness. If the instantaneous forces in the ligaments are compared at 10 percent strain, then the rank of ligaments from stiffest to least stiff is: TiC, ATiF, PTiF, CF, PTT, ATaF, ATT, and PTaF. If the instantaneous strains are compared at an arbitrary

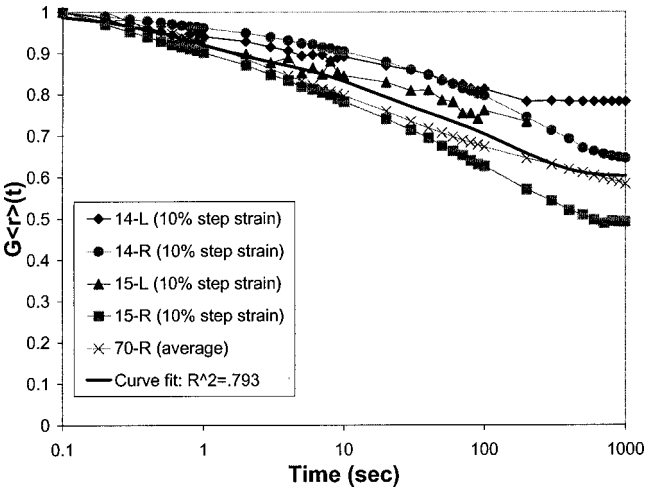

Fig. 6 Reduced relaxation function $G(t)$ data and curve fit for the posterior tibiofibular (PTiF) ligament ($n=5$). Inter-specimen variability was fairly low for this ligament type ($R^2 = 0.793$).

Table 2 Elastic response function curve-fit data

Ligament	A (N)	B	R^2
ATaF	7.18	12.50	0.965
ATiF	5.52	22.63	0.779
ATT	2.06	20.11	0.989
CF	0.20	49.63	0.828
PTaF	0.14	44.35	0.983
PTiF	6.87	20.07	0.275
PTT	1.34	28.65	0.999
TiC	0.51	45.99	0.543

Table 3 The relaxed length, unpreconditioned scale factor, failure loads, and failure test sample size for all ligament types. Values given as a mean±standard deviation.

Ligament	Relaxed length (mm)	Unpreconditioned scale factor (USF)	Failure load (N)	Failure test sample size
ATaF	11.00 ± 3.61	1.75 ± .71	297.1 ± 80.3	n=2
ATiF	7.17 ± 2.56	1.44 ± .32	708.1	n=1
ATT	12.00 ± 2.00	1.40 ± .29	130.8 ± 2.00	n=2
CF	24.67 ± 5.51	1.96 ± .45	598.0 ± 52.7	n=2
PTaF	15.33 ± 4.04	1.65 ± .14	554.2 ± 94.6	n=2
PTiF	9.80 ± 1.10	1.38 ± .09	N/A	n=0
PTT	10.67 ± 3.79	1.72 ± .09	N/A	n=0
TiC	31.67 ± 3.51	1.62 ± .33	403.4	n=1

force of 100 N, then the rank of ligaments from stiffest to least stiff becomes: TiC, CF, ATiF, PTiF, PTaF, PTT, ATT, and ATaF. The rank of ligaments from strongest to weakest in terms of available failure data from this study is ATiF, CF, PTaF, TiC, ATaF, and ATT (Table 3).

Preconditioning Effects. Preconditioning was found to affect the short-time behavior of ligament relaxation, but not the long-time behavior. Ligament specimens were found to experience a higher peak force value in response to a given step strain before preconditioning as compared to after preconditioning. This effect is described by an unpreconditioned scale factor (USF), defined here as the ratio of the peak force in the unpreconditioned state to the peak force in the preconditioned state (Table 3). However, it was found that ligament specimens eventually relaxed to the same force level for a given step strain, regardless of whether they were in a preconditioned state or not. Furthermore, time constants were found to be similar regardless of the state of preconditioning.

Strain Independence of Relaxation Function. In several cases, step tests at low strains produced low forces, and the reduced relaxation functions had to be thrown out due to the high level of noise. In the five cases where data from multiple step responses at different strain levels were taken from a single specimen and the reduced relaxation functions were curve-fit together, the goodness of fit was generally good ($R^2 > 0.6$ in all cases). However, the reduced relaxation functions were not the same at every strain level for a given specimen. In general, the greater the strain level of the step, the greater the relative degree of relaxation over time. In four out of five specimens, the G_∞ value of the reduced relaxation function decreased with each level of increasing strain (Fig. 7). In one ATaF ligament, the G_∞ value remained fairly constant over the range of strains tested (10–20 percent). Overall, statistical analysis showed no significant ($p < 0.05$) differences in the values of G_∞ at 10 percent strain compared to either 15 or 20 percent strain. However, there was a significant difference ($p < 0.05$) between the values of G_∞ at 15 and 20 percent strain.

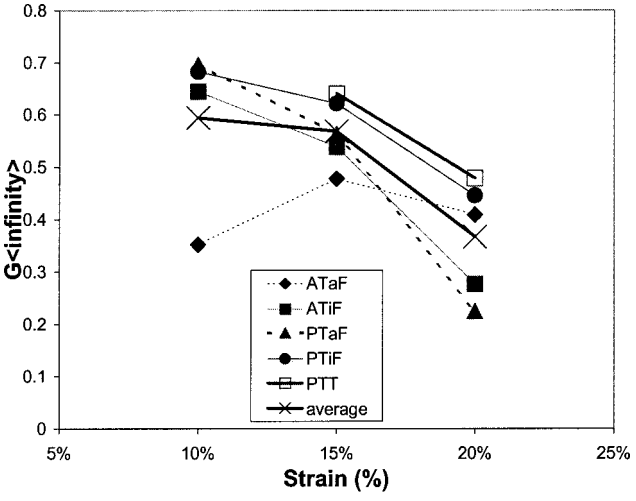

Fig. 7 G_∞ versus strain for serial step relaxation tests on the same specimen at various strain magnitudes. $N=1$ for each of the five ligament types. Statistically significant ($p<0.05$) differences were found between the values of G_∞ at 15 percent and 20 percent strain.

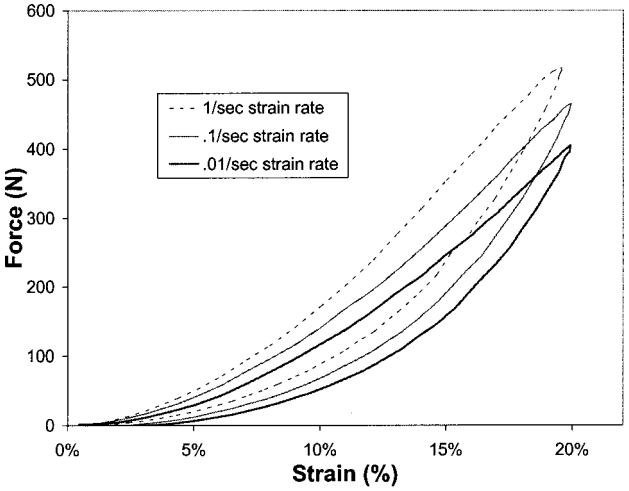

Fig. 8 Hysteresis loops for an anterior tibiofibular (ATiF) ligament specimen. The stiffness of the specimen is seen to increase at higher strain levels. Although stiffness also increases somewhat at higher strain rates, the data demonstrate that the ligament is not largely rate sensitive.

Rate Sensitivity. Hysteresis loops were plotted to evaluate the response of ankle ligaments to triangular waves applied at different ramp rates. A certain amount of strain-stiffening behavior was observed in all cases. However, there was very little difference in the hysteresis energy over the three decades of strain rates tested, even when testing to high forces and strains (Fig. 8). This confirms the observation by Woo et al. [3] and others that ligaments are generally rate-insensitive.

Discussion

This study characterized the viscoelastic properties of eight major ankle ligaments. The results of this study can be used to improve the constitutive modeling of ankle ligaments in computer models. When modeling biological systems computationally, the desired application of the model should govern the choice of the constitutive model. All constitutive models are an approximation of the actual mechanical behavior of the tissue of interest. Depending on the application, certain approximations may justify the use of a simpler or different constitutive model. Also, modeling software may be limited in the degree of complexity available for a constitutive model. Therefore, this study presents data that can be applied to several different constitutive models of varying degrees of complexity, including linear elastic, nonlinear elastic, linear viscoelastic, and quasi-linear viscoelastic (QLV) constitutive models.

Modeling of the Unpreconditioned State. In situations when the ankle is assumed to have remained motionless for a long period of time, it may be desirable to create a model of the ligaments in the unpreconditioned state. This can be done by linearly scaling the model parameters given in Tables 1 and 2. The elastic response function should be multiplied by the unpreconditioned scale factor USF, such that

$$A_{unpre} = A \cdot \mathrm{USF}$$

and B remains unchanged. The reduced relaxation function coefficients can also be linearly scaled to represent the ligament in an unpreconditioned state. G_1, G_2, and G_3 are scaled differently than G_∞, and τ_1, τ_2, and τ_3 remain unchanged:

$$G_{i_{unpre}} = \frac{G_i(\mathrm{USF} - G_\infty)}{\mathrm{USF}(1 - G_\infty)} \quad G_{\infty_{unpre}} = \frac{G_\infty}{\mathrm{USF}}$$

The observation that preconditioning only affects short-time viscoelastic behavior of ligaments is consistent with the hypothesis that preconditioning causes fluid exudation from the tissue, which in turn reduces the viscous component of the ligament's response [30].

Spring-Dashpot Configurations. Linear and nonlinear elastic and viscoelastic models can all be created using spring-dashpot configurations. Spring and dashpot parameters can be calculated from the elastic response and reduced relaxation function data (Tables 1 and 2). Strain ε can be converted into displacement x by using the relation $\varepsilon = x/L_0$, where L_0 is the relaxed ligament length (Table 3). A linear elastic model consists only of a spring. Therefore, the spring constant should be selected such that:

$$k(x) = F/x = \frac{A}{x}(e^{Bx/L_0} - 1)$$

at the reference displacement level x of interest. This equation is itself the spring function for a nonlinear elastic model.

Viscoelastic models will include dashpots. The linear viscoelastic model shown in Fig. 2 can be transformed into a quasi-linear model by making the spring and dashpot parameters nonlinear functions with respect to displacement. The spring functions can be calculated by multiplying the reduced relaxation function coefficients by the instantaneous force over displacement:

$$k_i(x) = \frac{G_i A}{x}(e^{Bx/L_0} - 1)$$

The dashpot functions should be modified accordingly to maintain the strain independence of the time constants:

$$\eta_i(x) = k_i \cdot \tau_i$$

The quasi-linear model can be made linear simply by applying these equations at some reference displacement x to obtain spring and damper constants. The reference displacement x should correspond to a strain level of interest, such as 10 percent strain.

Evaluation of Various Constitutive Models. Given these possible models, probably the most important degree of complexity to include in a constitutive model of any soft tissue, including human ankle ligament, is nonlinear elasticity. Almost all soft tissues exhibit a nonlinear elastic response to strain, beginning with an initial, soft ''toe region'' that is followed by a progressively stiffer ''loading region.'' Data from this study demonstrate that the elastic response of ankle ligament is highly nonlinear at a variety of loading rates (Fig. 8). A linear model is only accurate near the reference strain used in the model, and will not be accurate for strains even a few percent greater or less than the reference strain. Therefore, it is recommended that a nonlinear elastic response be modeled whenever possible.

An additional degree of complexity in the constitutive behavior of soft tissues is their viscoelasticity. To illustrate the difference in the behavior of the elastic and viscoelastic models, and linear and nonlinear models, ramp responses were calculated for all four models of the ATaF ligament at varying strain rates (Figs. 9(*a*) and 9(*b*)). Of course, the elastic models are insensitive to strain rate, because they represent an infinite strain rate. Fast strain rates (1/s) approximate the elastic response of most ankle ligaments in both the linear and quasi-linear viscoelastic models. Moderate (0.01/s) and slow (0.0001/s) strain rates produced considerably lower forces because they include a greater amount of relaxation.

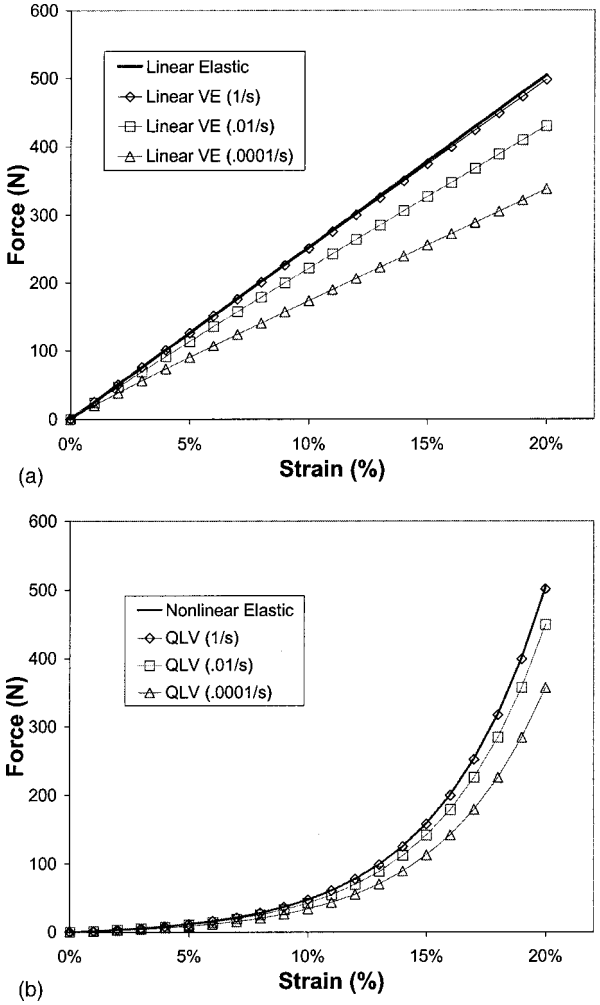

Fig. 9 (*a*) Linear elastic and viscoelastic models of the anterior tibiofibular (ATiF) ligament in response to ramp displacements at varying strain rates. In the linear models, the stiffness of the material stays constant or decreases with increasing strain, a characteristic not seen in the experimental data (see Fig. 8). (*b*) Nonlinear elastic and viscoelastic (QLV) models of the anterior tibiofibular (ATiF) ligament in response to ramp displacements at varying strain rates. The nonlinear models show an increasing stiffness in the material at higher strains, as seen in the expeirmental data (see Fig. 8).

Although viscoelasticity can have a considerable effect on ligament behavior, it may be neglected for very fast or very slow strain rates. At very fast strain rates ($>$ 1/s), there is not enough time for the ligament to relax appreciably, and the viscoelastic model approximates the elastic model. And at very slow strain rates ($<$ 0.0001/s), the ligament is almost fully relaxed throughout the event, and the viscoelastic model is essentially the elastic model scaled down by a factor of G_∞. Therefore, depending on the application of the model, it may not be necessary to include the viscoelastic component of ligament behavior. For example, computational models intending to study the lower extremity in an impact environment such as a car crash may be able to model ligament behavior realistically with a nonlinear, elastic constitutive model. In addition, for computer models focusing on the long-time behavior of ankle ligaments, such as distraction osteogenesis, a nonlinear elastic model may also be appropriate. How-

ever, for applications involving intermediate strain rates, such as gait analysis, the inclusion of a nonlinear viscoelastic model may be warranted.

Experimental Limitations. The data presented here is subject to experimental limitations at very fast and very slow strain rates. The accurate region of the reported relaxation function is bounded by the short and long time limits of the step relaxation test. The short time limit is the rise time of the applied step, which was effectively .1 s for data reported here, due to the contamination of short-time data from mechanical ringing of the test machine. The long time limit imposed on the experimental data is the hold time of the step relaxation test, which is 1000 seconds in the data presented here. Any time constants shorter than .1 seconds or longer than 1000 seconds would not be apparent in the data presented here. These experimental limitations would tend to result in an underestimation of the elastic response and an overestimation of the fully relaxed force.

Previous investigators have derived complex algorithms to correct for the finite rise time seen in real step relaxation tests [31,32,26,7]. These algorithms assume a strain history for the rise time portion of the test, typically a ramp. The method used in this study to correct for the finite rise time of the step was simply back-extrapolation of the relaxation function curve-fit. The back-extrapolation technique implicitly assumes the strain history of an ideal step applied at time zero. In reality, the strain history of an actual step relaxation test must include some sort of ramp during the rise time. However, the rise time of the ramp in this study was on the order of 0.02 s, so the strain history more closely resembled an ideal step with an instantaneous rise at time zero than it did a ramp with a rise time of 0.1 s. In addition, given that back-extrapolated peak forces were almost always less than 5 percent greater than the force values recorded at 0.1 s, error from back-extrapolation is likely to be small.

In addition to time limitations imposed on the data, there are strain limitations, as well. One possible error in strain measurement may derive from the fact that bone-ligament-bone samples were used in these tests. Woo et al. [3] noted that the total strain experienced by the bone-ligament-bone complex may not be identical to the strain experienced by the ligament alone. However, the difference is probably very small given that the elastic modulus of bone (~20 GPa) [33] is on the order of 100 times greater than the elastic modulus of most ankle ligaments (~200 MPa) [11]. Moreover, the bone–ligament–bone complex represents a functional unit whose behavior may actually be more applicable to computer models than the behavior of the ligament substance alone.

Accurate strain measurement may also have been compromised by methodological weaknesses. For example, the ligament specimens in this study were kept moist during testing by wrapping them in gauze soaked in PBS at room temperature. Placing them in a 37°C bath of PBS may have simulated in vivo conditions more closely [30]. Also, allowing a recovery time at least ten times greater than the hold time of the relaxation tests may have led to more repeatable results [23]. In addition, the use of a smaller test machine may have reduced or eliminated the problem of mechanical ringing contaminating the test data. In spite of these methodological shortcomings, the data presented here are in general agreement with the literature and represent the only published viscoelastic characterization of any human ankle ligament.

It should be noted that while most of the elastic response function curve-fits are valid up to 20 percent strain, the elastic response functions given for the CF, PTaF, and TiC ligaments are only valid up to 10 percent strain due to a lack of data beyond that strain level. Extrapolation beyond these strain levels will likely result in an overestimation of the ligament force. Obviously, none of the elastic response functions is valid when extrapolating past the failure force of the ligament.

The assumption that relative relaxation is independent of step strain level may not be valid at all strain levels of interest. Statistical results suggest that the average value of G_∞ can be assumed to remain constant only up to 15 percent strain at most (Fig. 7). Although this calculation is based on a small number of samples, it is likely that the quasi-linear model of viscoelasticity is only theoretically valid up to a certain strain level. Beyond that strain level, a fully nonlinear model may be required to adequately describe the data.

Failure Data. Failure loads reported in this study are quite a bit higher than what has been previously reported in the literature. For example, Attarian et al. [10] reported average ultimate loads of 138.9 N for the ATaF, 345.7 N for the CF, and 261.2 N for the PTaF. Siegler et al. [11] reported failure loads of 231 N for the ATaF, 307 N for the CF, and 418 N for the PTaF. Parenteau et al. [15] reported failure loads of 0–286 N for the ATaF, 120–290 N for the CF, 307 N for the PTaF, and 467 N for the PTT. All of these failure strengths are lower than the failure loads reported in this study (Table 3). One possible explanation for this difference is that our specimens came from 50th percentile, middle-aged male donors, as opposed to older, smaller and/or female donors. Also, failure tests in this study were performed at a fast rate (~280 mm/s), as opposed to the quasi-static rates used by Siegler et al. [11] and Parenteau et al. [15]. Unfortunately, cutting and drilling the bone ends of each specimen caused most of them to fail at the potting, reducing the sample size of successful failure tests considerably.

Conclusions

This study has produced data for modeling the behavior of eight major ankle ligaments at a wide variety of strains and strain rates. Failure data was reported, as well as a method to model the ligaments in an unpreconditioned state. All ankle ligaments were found to be nonlinear viscoelastic. Nonlinear constitutive models are recommended for every application, and viscoelastic constitutive models are recommended for applications involving strain rates between 1/s and 0.0001/s. The quasi-linear model was found to be valid up to 15 percent strain. It is anticipated that the addition of quasi-linear viscoelastic ankle ligaments will improve the biofidelity of computational models of the lower extremity.

Acknowledgments

The authors gratefully acknowledge Dr. Borjana Mikic for providing access to the material testing equipment in the Orthopaedic Biomechanics Laboratory at UVa. The authors also thank Sue George and Bryan Bush for their assistance with the experiments. This research was funded in part by DOT NHTSA Contract No. DTNH22-93-Y-07028.

References

[1] Viidik, A., 1966, ''Biomechanics and Functional Adaptation of Tendons and Joint Ligaments,'' F. G. Evans, ed., in *Studies on the Anatomy and Function of Bone and Joints*, Springer, Berlin, pp. 17–39.
[2] Fung, Y. C., 1981, *Biomechanics: Mechanical Properties of Living Tissues*, Springer-Verlag, New York.
[3] Woo, S. L.-Y., Gomez, M. A., and Akeson, W. H., 1981, ''The Time and History-Dependent Viscoelastic Properties of the Canine Medial Collateral Ligament,'' ASME J. Biomech. Eng., **103**, pp. 293–298.
[4] Lam, T. C., Frank, C. B., and Shrive, N. G., 1993, ''Changes in the Cyclic and Static Relaxations of the Rabbit Medial Collateral Ligament Complex During Maturation,'' J. Biomech., **26**, No. 1, pp. 9–17.
[5] Thornton, G. M., Oliynyk, A., Frank, C. B., and Shrive, N. G., 1997, ''Ligament Creep Cannot Be Predicted From Stress Relaxation at Low Stress: A Biomechanical Study of the Rabbit Medial Collateral Ligament,'' J. Orthop. Res., **15**, pp. 652–656.
[6] Quapp, K. M., and Weiss, J. A., 1998, ''Material Characterization of Human Medial Collateral Ligament,'' ASME J. Biomech. Eng., **120**, pp. 757–762.
[7] Kwan, M. K., Lin, T. H.-C., and Woo, S. L.-Y., 1993, ''On the Viscoelastic Properties of the Anteromedial Bundle of the Anterior Cruciate Ligament,'' J. Biomech., **26**, Nos. 4 and 5, pp. 447–452.
[8] Soslowsky, L. J., An, C. H., DeBano, C. M., and Carpenter, J. E., 1996, ''Coracoacromial Ligament: In Situ Load and Viscoelastic Properties in Rotator Cuff Disease,'' Clin. Orthop. Relat. Res., **330**, pp. 40–44.
[9] Yahia, L. H., Audet, J., and Drouin, G., 1991, ''Rheological properties of the human lumbar spine ligaments,'' J. Biomed. Eng., **13**, No. 5, pp. 399–406.

[10] Attarian, D. E., McCrackin, H. J., DeVito, D. P., McElhaney, J. E., and Garrett, W. E., 1985, ''Biomechanical Characteristics of Human Ankle Ligaments,'' Foot & Ankle, **6**, No. 2, pp. 54–58.
[11] Siegler, S., Block, J., and Schneck, C. D., 1988, ''The Mechanical Characteristics of the Collateral Ligaments of the Human Ankle Joint,'' Foot & Ankle, **8**, No. 5, pp. 234–242.
[12] Begeman, P., and Aekbote, K., 1996, ''Axial Load Strength and Some Ligament Properties of the Ankle Joint,'' *Proceedings of the Injury Prevention Through Biomechanics Symposium*, pp. 125–135.
[13] Hurwitz, S. R., 1995, ''Clinical Aspects of Foot/Ankle Injuries,'' presented at the International Conference on Pelvic and Lower Extremity Injuries (PLEI).
[14] Klopp, G. S., Crandall, J. R., Hall, G. W., and Pilkey, W. D., 1997, ''Foot and Ankle in Dynamic Axial Impacts to the Foot,'' *Proceedings of the International IRCOBI Conference*, Hannover, Germany.
[15] Parenteau, C. S., Viano, D. C., and Petit, P. Y., 1998, ''Biomechanical Properties of Human Cadaveric Ankle-Subtalar Joints in Quasi-Static Loading,'' ASME J. Biomech. Eng., **120**, pp. 105–111.
[16] Hall, G. W., Thunnissen, J. R., Crandall, J. R., and Pilkey, W. D., 1998, ''Development of a Multibody Dynamic Model to Analyze Human Lower Extremity Impact Response and Injury,'' *Proceedings of the International IRCOBI Conference*, pp. 117–134.
[17] Tannous, R. E., Bandak, F. A., Toridis, T. G., and Eppinger, R. H., 1996, ''A Three-Dimensional Finite Element Model of the Human Ankle: Development and Preliminary Application to Axial Impulsive Loading,'' SAE 962427, *Proceedings of the 40th Stapp Car Crash Conference*, pp. 219–238.
[18] Allard, P., Thiry, P. S., and Duhaime, M., 1985, ''Estimation of the Ligament's Role in Maintaining Foot Stability Using a Kinematic Model,'' Med. Biol. Eng. Comput., **23**, pp. 237–242.
[19] Schauer, D. A., Benda, B., Weiss, J., Perfect, S., Moor, E., II, and Kleinberger, M., 1995, ''Lower Extremity Finite Element Model Development,'' *Proceedings of the International Conference on Pelvic and Lower Extremity Injury* (PLEI).
[20] Bedewi, P. G., and Bedewi, N. E., 1996, ''Modelling of Occupant Biomechanics With Emphasis on the Analysis of Lower Extremity Injuries,'' Int. J. Crashworthiness, **1**, No. 1, pp. 50–72.
[21] Scott, S. H., and Winter, D. A., 1993, ''Biomechanical Model of the Human Foot: Kinematics and Kinetics During the Stance Phase of Walking,'' J. Biomech., **26**, No. 9, pp. 1091–1104.
[22] Beaugonin, M., Haug, E., and Cesari, D. 1997, ''Improvement of Numerical Ankle/Foot Model: Modeling of Deformable Bone,'' SAE 973331, *Proceedings of the 41st Stapp Car Crash Conference*, Lake Buena Vista, FL, pp. 225–249.
[23] Pradas, M. M., and Calleja, R. D., 1990, ''Nonlinear Viscoelastic Behavior of the Flexor Tendon of the Human Hand,'' J. Biomech., **23**, No. 8, pp. 773–781.
[24] Ray, R. G., Christensen, J. C., and Gusman, D. N., 1997, ''Critical Evaluation of Anterior Drawer Measurement Methods in the Ankle,'' Clin. Orthop. Relat. Res., **334**, pp. 215–224.
[25] Gerber, J. P., 1998, ''Persistent Disability Associated With Ankle Sprains: A Prospective Examination of an Athletic Population,'' *Proceedings of the American Orthopaedic Foot and Ankle Society (AOFAS) Winter Meeting*, New Orleans, LA, Mar. 22.
[26] Myers, B. S., McElhaney, J. H., and Doherty, B. J., 1991, ''The Viscoelastic Responses of the Human Cervical Spine in Torsion: Experimental Limitations of Quasi-Linear Theory, and a Method for Reducing These Effects,'' J. Biomech., **24**, No. 9, pp. 811–817.
[27] Woo, S. L.-Y., Simon, B. R., Kuei, S. C., and Akeson, W. H., 1980, ''Quasi-Linear Viscoelastic Properties of Normal Articular Cartilage,'' ASME J. Biomech. Eng., **102**, pp. 85–90.
[28] Green, A. E., and Rivlin, R. S., 1957, Arch. Ration. Mech. Anal., **1**, pp. 1–21.
[29] Parham, K. R., Gordon, C. C., and Bensel, C. K., 1992, *Anthropometry of the Foot and Lower Leg of U.S. Army Soldiers: Fort Jackson, SC-1985*, United States Army Natick Research, Development and Engineering Center, Natick, MA.
[30] Chimich, D., Shrive, N., Frank, C., Marchuk, L., and Bray, R., 1992, ''Water Content Alters Viscoelastic Behavior of the Normal Adolescent Rabbit Medial Collateral Ligament,'' J. Biomech., **25**, No. 8, pp. 831–837.
[31] Dortmans, L. J. M. G., Sauren, A. A. H. J., and Rousseau, E. P. M., 1984, ''Parameter Estimation Using the Quasi-Linear Viscoelastic Model Proposed by Fung,'' ASME J. Biomech. Eng., **106**, pp. 198–203.
[32] Nigul, I., and Nigul, U., 1987, ''On Algorithms of Evaluation of Fung's Relaxation Function Parameters,'' J. Biomech., **20**, No. 4, pp. 343–352.
[33] Turner, C. H., Rho, J., Takano, Y., Tsui, T. Y., and Pharr, G. M., 1999, ''The Elastic Properties of Trabecular and Cortical Bone Tissues Are Similar: Results From Two Microscopic Measurement Techniques,'' J. Biomech., **32**, pp. 437–441.